Cofactor Requirements and Reconstitution Of Microcin B17 Synthetase: A Multienzyme Complex that Catalyzes the Formation of Oxazoles and Thiazoles in the Antibiotic Microcin B17†

Jill C. Milne,‡ Ranabir Sinha Roy,‡ Andrew C. Eliot, Neil L. Kelleher, Anita Wokhlu, Bryce Nickels, and Christopher T. Walsh*

Department of Biological Chemistry and Molecular Pharmacology, Harvard Medical School, Boston, Massachusetts 02115

Received December 17, 1998

ABSTRACT: In the maturation of the *Escherichia coli* antibiotic Microcin B17 (MccB17), the McbA prepro-antibiotic is modified post-translationally by the multimeric microcin synthetase complex (composed of the McbB, -C, and -D proteins), which cyclizes four cysteines and four serines to thiazoles and oxazoles, respectively. Herein, we report the purification of individual subunits of MccB17 synthetase as fusions to maltose binding protein (MBP), and the in vitro reconstitution of heterocyclization activity. Preliminary characterization of each subunit reveals McbB to be a zinc-containing protein that may catalyze the initial cyclodehydration step, and McbC to contain flavin, consistent with an anticipated role for a dehydrogenase. We have previously demonstrated that McbD is a regulated ATPase/GTPase that may function as a conformational switch. Photolabeling experiments with the McbA propeptide now identify McbD as the initial site of substrate recognition. Heterocyclization activity was reconstituted only by combining all three subunits, demonstrating that each protein is required for heterocycle formation. Titration assays indicate that the subunits bind to each other with at least micromolar affinities, although McbD affords activity only after the MBP tag is proteolytically removed. Subunit competition assays with an $McbD_{D147A}$ mutant, which yields a catalytically deficient synthetase in vivo, show it to be defective in complex formation, whereas the $McbB_{C181A/C184A}$ double mutant, which is also inactive, competitively inhibits reconstitution by native McbB. Addition of the HtpG chaperone (originally shown to copurify with MccB17 synthetase), does not stimulate synthetase reconstitution or heterocyclization activity in vitro. A model for synthetase activity is proposed.

A large number of natural products contain one or more of the five-membered oxazole and thiazole heterocycles (or the corresponding dihydro oxazolines and thiazolines), which are derived from precursor peptides containing Xaa-Ser/Thr/Cys sequences (*1*). These natural products are produced by diverse organisms and exhibit a broad spectrum of biological activity of demonstrable therapeutic value. For example, bleomycin A (*2*), a widely prescribed anticancer drug, effects the oxidative degradation of DNA and uses a bithiazole moiety to bind its target DNA sequences (*3*, *4*). Bacitracin (*5*), a thiazoline-containing peptide antibiotic, interdicts bacterial cell wall biosynthesis by complexation with C_{55}-bactoprenolpyrophosphate (*6*). Yersiniabactin (*7*) and exochelin (*8*) are siderophores that exploit the metal (Fe^{III}) coordinating properties of thiazolines and oxazolines, and serve as virulence factors in the producing pathogens (*Yersinia pestis* and *Mycobacterium tuberculosis*, respectively). Thiangazole (*9*) contains a tandem array of one oxazole and three thiazolines and exhibits antiviral activity (*10*). Yet other oxazole/thiazole-containing natural products such as thiostrepton (*11*) and GE2270A (*12*) inhibit translation steps in bacterial protein synthesis.

Certain strains of *Escherichia coli* produce a peptide antibiotic, Microcin B17 (MccB17) (*13*), which is profusely decorated with oxazoles and thiazoles (*14*, *15*). MccB17 is ribosomally synthesized, and genetic studies have implicated bacterial DNA gyrase as its cellular target (*16*). Biosynthesis and secretion of MccB17 require a plasmid-encoded operon containing seven genes (*mcbABCDEFG*) (*17*). The *mcbA* gene encodes a 69 amino acid prepro-antibiotic (*18*). McbB, -C, and -D are required for the maturation of McbA to the thiazole- and oxazole-containing proMccB17 (Figure 1) (*19*). The N-terminal 26 residues of proMccB17 are removed by an as yet unidentified protease, and the mature MccB17 containing eight heterocycles (four oxazoles and four thia-

† This research was supported by NIH Grant GM 20011 to C.T.W. J.C.M. is an American Cancer Society Postdoctoral Research Fellow (Grant No. PF4332). R.S.R. is a Parke-Davis Fellow of the Life Sciences Research Foundation. N.L.K. is an NIH postdoctoral fellow.

‡ These authors contributed equally to this work.

* To whom correspondence should be addressed. Phone: 617-432-1715. Fax: 617-432-0556. E-mail: walsh@walsh.med.harvard.edu.

[1] Abbreviations: BPA, L-4-benzoylphenylalanine; CBP, calmodulin binding peptide; Da, Daltons; DTT, dithiothreitol; EDTA, ethylenediaminetetraacetic acid; ESI/FTMS, electrospray ionization Fourier transform mass spectrometry; HRP, horseradish peroxidase; ICP-AAS, inductively coupled plasma atomic absorption spectroscopy; IPTG, isopropyl-1-thio-β-D-galactosidase; LB, Luria-Bertani medium; MBP, maltose binding protein; MccB17, Microcin B17; MS, mass spectrometry; Nle, L-norleucine; PAGE, polyacrylamide gel electrophoresis; PCR, polymerase chain reaction; PNP, L-*p*-nitrophenylalanine; PMSF, phenylmethanesulfonyl fluoride; RP-HPLC, reversed-phase high-pressure liquid chromatography; UV, ultraviolet; WT, wild-type.

10.1021/bi982975q CCC: $18.00
Published on Web 03/20/1999

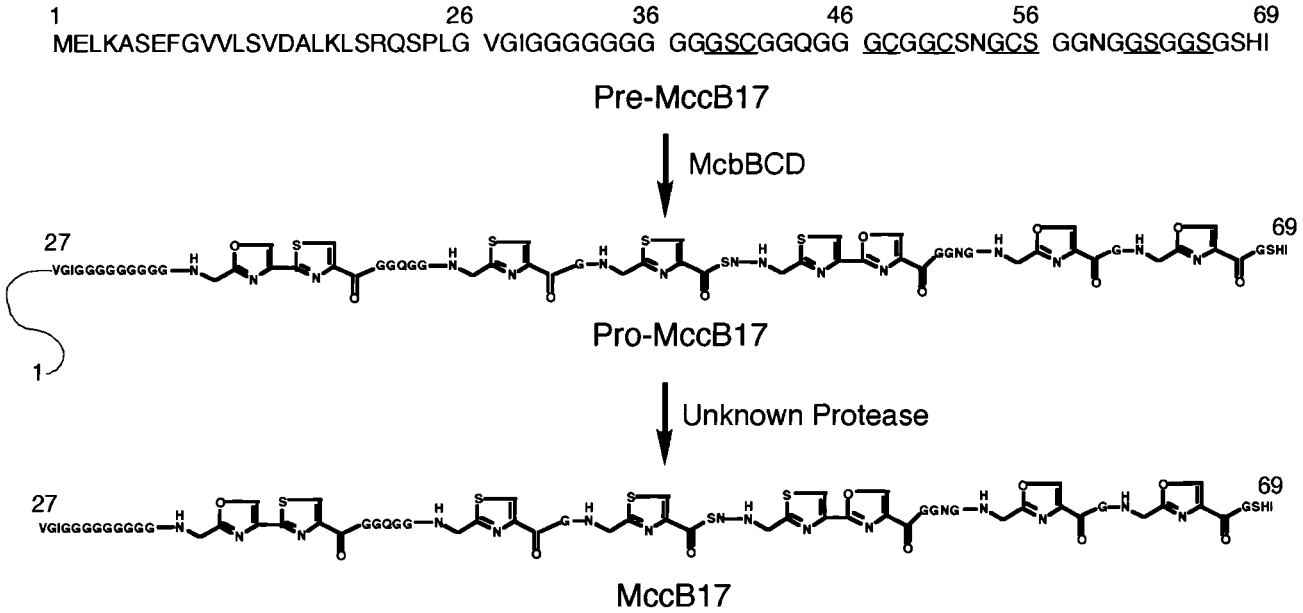

FIGURE 1: Maturation of MccB17. The 69 residue pre-MccB17 is processed by MccB17 synthetase to pro-MccB17 incorporating eight heterocycles (four oxazoles and four thiazoles). Residues that are modified are underlined. The *N*-terminal 26 amino acid propeptide (leader) sequence is removed by an unknown *E. coli* protease to release mature MccB17.

zoles) is secreted by McbE and -F, which function as an ABC-type transporter (*20*). McbG is an immunity protein of undefined mechanism, which protects the producing cell from the cytotoxic activity of MccB17 (*20*).

To date, MccB17 is the only system for which the enzymes responsible for post-translational heterocycle formation have been identified and cloned (*21*). Genetic analyses showed that coexpression of *mcbA* and *mcbBCD* led to the production of active MccB17 and that strains carrying a null mutation in any one of *mcbB*, *mcbC*, or *mcbD* were unable to modify McbA (*22*). We subsequently reported the purification of a MccB17 synthetase complex containing the three subunits McbB, -C, and -D (*23*), and demonstrated heterocyclization activity in vitro, allowing the opportunity to gain insight into the mechanism of peptide-based oxazole and thiazole biosynthesis.

In an attempt to deconvolute the recognition processes involved in peptidyl heterocyclization, we have probed issues of substrate specificity for the synthetase. We have noted an absolute requirement for a propeptide sequence in McbA (residues 1−26), fused in cis and upstream of a heterocyclizable di- or tripeptide moiety (e.g., Gly^{39}-Ser^{40}-Cys^{41}) via a polyglycine linker comprising at least five glycines (*24*, *25*). This prerequisite defines the minimal substrate fragment to encompass at least the first 40 residues of McbA. Subsequent in vitro studies with $McbA_{1-46}$ analogues as substrates have investigated the chemoselectivity and regioselectivity of heterocyclization (*26*, *27*) and the local sequence context of cyclizable Ser and Cys residues (*25*).

A key observation for demonstrating MccB17 synthetase activity was its requirement for ATP in the heterocyclization process (*23*). We have recently shown that the McbD subunit incorporates a motif that is reminiscent of the Walker B box in ATP utilizing enzymes and of motifs found in small G protein GTPases (*28*). Mutation of several of the key residues in this motif reduces MccB17 production in vivo and substrate turnover in vitro, suggesting that McbD may possess a regulated ATPase/GTPase domain necessary for peptide heterocyclization.

A delineation of the precise roles played by the individual McbB, -C, and -D subunits in oxazole and thiazole formation and the identification of additional cofactors that may be enlisted by the synthetase have been hampered by low expression levels and by the copurification of subunits as a multimeric complex, even after multistep chromatography. We have therefore focused on isolating each subunit protein in milligram quantities for analyses of structure and function. The success of such an approach, however, depends on the ability to reconstitute heterocyclization activity from the isolated proteins, since activity assays for the individual subunits have not yet been devised. In this report we describe the overexpression and purification of each of the subunits of MccB17 synthetase, McbB, McbC, and McbD, as fusions to maltose binding protein (MBP), and demonstrate initial reconstitution of MccB17 synthetase activity in vitro with these purified components. Preliminary analysis of the individual subunits has identified McbB as a zinc-containing protein, McbC as a flavoprotein, and McbD as the site of recognition for the propeptide region of the McbA substrate.

EXPERIMENTAL PROCEDURES

Materials. Bacteriological media were obtained from Difco Laboratories. Competent *E. coli* strain BL21(DE3) {F^-, *ompT*, *hsdS*$_B$, (r_B^-, m_B^-), *gal*, *dcm*, (DE3)}, thrombin, and His-bind resin were obtained from Novagen. Competent *E. coli* strain DH5α {F^-, ϕ80d*lacZ*Δ*M*15, Δ(*lac*ZYA-*arg*F)-U169, *deo*R, *rec*A1, *end*A1 *hsd*R17(r_K^-, m_K^+), *pho*A, *sup*E44, λ^-, *thi*-1, *gyr*A96, *rel*A1} and plasmid pUC19 were purchased from Gibco BRL. The *htpG* knockout *E. coli* strain MC4100Δ*htpG* has been described earlier (*23*). Restriction endonucleases, T4 DNA ligase, dNTPs, and amylose resin were obtained from New England Biolabs. Isopropyl-1-thio-β-D-galactopyranoside (IPTG) was purchased from Bachem Biosciences. Kanamycin, ampicillin, and benzamidine were obtained from Sigma. Low molecular weight markers were obtained from Bio-Rad. Biotinylated markers were obtained from Tropix. The purification of wild-type MccB17 syn-

thetase by multistep chromatography and the affinity purification of the calmodulin binding peptide (CBP)-tagged synthetase complex (CBP tag on McbB) have been reported earlier (*23*, *25*).

Substrates. The polypeptide PNP-McbA$_{1-46}$ (NH_2-PNP-Nle-McbA$_{2-46}$-$CONH_2$), used as a substrate in certain MccB17 synthetase assays, was synthesized using solid-phase Fmoc-based peptide synthesis on an automated peptide synthesizer (R. Sinha Roy and C. T. Walsh, unpublished experiments). This minimal substrate incorporates the first bisheterocyclization site of McbA (Gly^{39}-Ser^{40}-Cys^{41}), and a *p*-nitrophenylalanine (PNP) residue at the N-terminus (ϵ_{280} = 9340 M^{-1} cm^{-1}) to facilitate accurate quantitation of peptide concentration by UV−vis spectroscopy. The other substrates used are MBP-McbA$_{1-46(GGC)}$ ("GGC"), an S40G variant of McbA$_{1-46}$ that contains only one potential site for heterocyclic modification fused downstream of maltose binding protein (MBP), and full-length McbA fused either to an upstream hexahistidine affinity tag (His_6-McbA) or to maltose binding protein (MBP-McbA). All of these substrates are efficiently processed by the synthetase in vitro. The synthetic polypeptide McbA$_{1-26}$-$CONH_2$, which encompasses the propeptide sequence of McbA (residues 1−26), has been described earlier (*29*). The propeptide analogue biotinyl-F8BPA, which is a biotinylated McbA$_{1-26}$ analogue containing L-4-benzoylphenylalanine (BPA) instead of Phe^8 was synthesized by QCB Inc. (Hopkinton, MA). This peptide has a biotin moiety appended to the N-terminus via an ϵ-aminocaproic acid linker to enable detection by avidin-based techniques. The construction of GGC, His_6-McbA, and MBP-McbA has been reported earlier (*23*, *26*, *28*).

Recombinant DNA Methods. Recombinant DNA techniques were performed as described elsewhere (*30*). Preparation of plasmid DNA, gel purification of DNA fragments, and purification of polymerase chain reaction (PCR) amplified products were performed using a QIAprep spin plasmid kit, a QIAEX II gel extraction kit, and a QIAquick PCR purification kit, respectively (Qiagen). Oligonucleotide primers were obtained from Integrated DNA Technologies or Gene Link. PCR reactions were performed in 100 μL volumes containing 1 × *Pfu* polymerase reaction buffer (Stratagene), 200 μM each dNTP, 1 μM each PCR primer, approximately 200 ng of plasmid template, and 2.5 units of cloned *Pfu* polymerase. The fidelity of PCR products was confirmed by nucleotide sequencing after subcloning into the appropriate expression vector. DNA sequencing was performed by the Molecular Biology Core Facility of the Dana Farber Cancer Institute (Boston, MA) and the Biopolymers Facility in the Department of Biological Chemistry and Molecular Pharmacology at Harvard Medical School.

Construction of MBP-McbB, MBP-McbC, and MBP-McbD. The expression vectors for the MBP-McbB (pETMBP-McbB) and MBP-McbC (pETMBP-McbC) fusion proteins were constructed from plasmids pET15b-McbB (J. C. Milne and C. T. Walsh, unpublished experiments) and pET15b-McbC (*23*), which are pET15b (Novagen) derivatives that encode hexa-histidine-tagged McbB and McbC, respectively. Briefly, the sequences coding for the hexahistidine tag (*Nco*I-*Nde*I) were replaced by the *Nco*I-*Nde*I fragment from plasmid pIADL14 (*31*), which encodes maltose binding protein followed by a thrombin cleavage site (LVPRGS). The McbB mutants McbB$_{C181A/C184A}$, McbB$_{C266A/C269A}$, and McbB$_{C181A/C184A/C266A/C269A}$ were constructed using plasmids pETMBP-McbB and pUC19Mccb17 (*28*) as templates. The latter incorporates the entire *mccB17* operon into the pUC19 vector. Mutagenesis was performed using the QuikChange site-directed mutagenesis kit (Stratagene). For expression, the plasmids were transformed into *E. coli* strain BL21(DE3).

To construct the expression vector for the MBP-McbD fusion protein (pETMBP-McbD), the coding sequence of *mcbD* was amplified by PCR from plasmid pPY113 (*19*), which contains the entire *mccB17* operon cloned into pBR322. The primers 5′-GATCGATCGGATCCATGATAAATGTCTACAGTAAC-3′ and 5′-AAGCTTTTATGGGAATGGTACC-3′ introduced a *Bam*HI site at the 5′ end and a *Hin*dIII site at the 3′ end, respectively. The PCR product was digested with *Bam*HI and *Hin*dIII and ligated with plasmid pIADL14 cut with the same enzymes.

The D147A mutation in pETMBP-*mcb*D was constructed by PCR amplification using the template plasmid pUC19-MccB17(D147A), which incorporates this mutation into the native *mccB17* operon (*28*). Briefly, the coding sequence of the mutant mcbD fragment was PCR amplified from the template using the same 3′ and 5′ PCR primers as above. The PCR product was digested with *Bam*HI and *Hin*dIII and ligated with pIADL14 cut with *Bam*HI and *Hin*dIII to afford plasmid pETMBP-McbD$_{D147A}$. For expression of MBP-McbD and MBP-McbD$_{D147A}$, the corresponding pET plasmids were transformed into *E. coli* strain BL21(DE3).

Overexpression and Purification of MccB17 Synthetase Subunits. For expression of MBP-McbB and its mutants, MBP-McbC and McbD$_{D147A}$, 10 mL of an overnight culture of the expression strain was used to inoculate 1 L of LB-ampicillin (100 μg/mL). MBP-McbD was similarly expressed in 1 L of LB-kanamycin (50 μg/mL). Cultures were grown at 37 °C and induced with 1 mM IPTG at an OD_{600} of 0.6−0.8. After 3 h (MBP-McbB and MBP-McbC) or 0.5−1 h (MBP-McbD) of induction, the cells were harvested by centrifugation and resuspended in 20 mL of buffer A (20 mM Tris−HCl, pH 7.5, 200 mM NaCl). The cells were disrupted twice in a French pressure cell (18 000 psi), and cellular debris was removed by centrifugation (18000*g*, 30 min). The supernatant was applied to an amylose column (15−20 mL bed volume). The column was washed with 20 column volumes of buffer A, and the MBP fusion protein was eluted with buffer B (20 mM Tris, pH 7.5, 200 mM NaCl, and 10 mM maltose). Fractions (5 mL each) containing the protein were combined, concentrated in a Centriprep 30 concentration unit (Millipore), aliquoted, and stored at −80 °C. Protein concentration was determined by UV−vis spectroscopy, and extinction coefficients were calculated on the basis of a modification of the Edelhoch method (*32*, *33*) (ϵ_{280} = 112 760 M^{-1} cm^{-1} for MBP-McbB, 96 720 M^{-1} cm^{-1} for MBP-McbC, and 120 670 M^{-1} cm^{-1} for MBP-McbD).

Construction of pET15b-htpG. *htpG* was cloned by colony PCR using strain ZK4 as template with the appropriate restriction sites introduced by the reverse (5′-GATCGATCCATATGAAAGGACAAGAAACTCGTGGT-3′) and forward (5′-GATCGATCGGATCCTCAGGAAACCAGCAGCTGGTTCAT-3′) PCR primers (*Bam*HI and *Nde*I, respectively). The PCR product was digested with *Nde*I and *Bam*HI and ligated to pET15b cut with the same restriction enzymes. The ligation reactions were transformed into *E. coli* DH5α.

The purified plasmid, pET15b-HtpG, was then transformed into the *E. coli* expression host, BL21(DE3).

Overexpression and Purification of His$_6$-HtpG. The recombinant protein expressed from BL21(DE3)/pET15b-HtpG is produced with an amino-terminal hexa-histidine (His_6) tag, allowing the protein to be purified by affinity chromatography on a Ni^{2+} His-bind column. Briefly, cultures of BL21-(DE3)/pET15b-HtpG were grown in LB-ampicillin (100 μg/mL) to an OD_{600} of 0.6−1.0, and protein expression was induced by addition of IPTG (1mM). After 3 h of induction, the cells were harvested by centrifugation and resuspended in 20 mL of binding buffer (20 mM Tris, pH 7.5, 200 mM NaCl). The cells were disrupted twice in a French pressure cell (18 000 psi), and cellular debris was removed by centrifugation (18000*g*, 30 min). The supernatant was applied to a His-bind Ni^{2+} column (15−20 mL bed volume). The column was washed with binding buffer (20 mM Tris−HCl, pH 7.9, 5 mM imidazole, 500 mM NaCl, 10 column volumes) and then with wash buffer (20 mM Tris−HCl, pH 7.9, 60 mM imidazole, 500 mM NaCl, 6 column volumes). The protein was eluted with elution buffer (10 mM Tris−HCl, pH 7.9, 500 mM imidazole, 250 mM NaCl, 6 column volumes) and dialyzed against 20 mM Tris, pH 7.5, 200 mM NaCl. After dialysis the protein was concentrated in a Centriprep 30 concentration unit (Millipore), aliquoted, and stored at −80 °C. Protein concentration was determined by UV−vis spectroscopy (ϵ_{280} = 81 820 M^{-1} cm^{-1}).

Metal Analysis. Adventitious metals were removed from buffers and slidealyzer dialysis cassettes (Pierce), pipet tips, and eppendorfs according to published procedures (*31*). MilliQ water and chelex-treated buffers were determined to be metal-free by inductively coupled plasma atomic absorption spectroscopy (ICP-AAS) analysis. For quantitation of metals, a solution of MBP-McbB (3−5 mg/mL) was dialyzed against 3−4 changes of metal-free buffer (50 mM HEPES, pH 8.0) over chelex resin (10 g/L). Samples were subsequently transferred to metal-free eppendorf tubes, frozen, and analyzed for metal content by ICP-AAS at the University of Georgia Chemical Analysis Laboratory (Athens, GA). Detection limits for zinc were determined to be <1 ppb.

Flavin Identification. The flavin was released from MBP-McbC by boiling for 15 min. The denatured protein was removed by centrifugation, and the flavin was identified by HPLC analysis (Vydac C18 column, solvent A = 0.1 M potassium phosphate, pH 5.3; solvent B = methanol, 10−40% B over 60 min). Solutions of FMN and FAD were used as standards for the HPLC analysis.

Western Blot Assay for Synthetase Activity. Reaction mixtures consisted of 20 μM GGC (unless otherwise noted), MccB17 synthetase buffer [50 mM Tris pH 7.5, 100 mM NaCl, 20 mM $MgCl_2$, 10 mM DTT, 2 mM ATP], and CBP-tagged MccB17 synthetase (0.05 μg/μL). Reactions were incubated at 37 °C, and aliquots were removed at the times indicated in the figure legends, quenched with SDS−PAGE sample buffer, and electrophoresed on a 10% SDS−PAGE gel (16% SDS−PAGE gel for PNP-McbA$_{1-46}$). The gels were transblotted to Immobilon-P PVDF membranes (Millipore) at 60 V for 60 min and analyzed by protein immunoblotting with rabbit polyclonal anti-MccB17 antibodies (*19*) and goat anti-rabbit Horseradish peroxidase-conjugated antibodies (IgG (H + L), Pierce). The anti-MccB17 antibodies have been shown to detect even a single oxazole or thiazole heterocycle out of the eight present in mature MccB17 (*25*). Immunoblots were developed on film (Reflection, Dupont New England Nuclear) using the chemiluminescent SuperSignal detection system (Pierce). The HRP substrate was diluted 1:5 with water and incubated with the immunoblot for 3 min to avoid signal saturation. Developed films were scanned and quantified using NIH image software (Version 1.61, NIH).

Photolabeling Experiments. The concentration of a biotinyl-F8BPA stock solution in 20% acetonitrile was determined by UV−vis spectroscopy using the extinction coefficient of 4-methylbenzophenone as a reasonable estimate for that of the BPA residue (ϵ_{264} = 17 378 M^{-1} cm^{-1}). For the determination of an IC_{50} value of biotinyl-F8BPA, increasing concentrations of the peptide (0−160 μM) were incubated with MBP-McbA (20 μM) and CBP-tagged synthetase (0.05 μg/μL) in synthetase buffer at 37 °C. After 30 min, the assays were quenched with SDS−PAGE gel loading buffer and analyzed by western immunoblots as described earlier. For the photolabeling experiment, biotinyl-F8BPA (12.5 μM) was incubated with synthetase (0.05 μg/mL) at 37 °C for 1 h and irradiated with UV−vis light (λ = 350 nm, 8 min, 4 °C). The McbB (33 kDa), McbC (31 kDa), and McbD (43 kDa) subunits were resolved by SDS−PAGE on a 7.5% gel and transblotted to a PVDF membrane as described earlier, and labeled subunits were detected by probing with HRP-conjugated avidin.

Thrombin Digestions. MBP fusion proteins (20 μM) were incubated with thrombin (protease units as indicated in the figure legends) for 15 min at room temperature. The digestions were quenched by adding benzamidine (2 mM final concentration) and incubating for 5 min at room temperature. The extent of cleavage was assessed by SDS−PAGE.

Bioassay for MccB17 Antibiotic Activity. Frozen stocks of *E. coli* DH5α/pUC19mccb17 wild-type and mutant strains were used to inoculate 2 mL cultures of LB-ampicillin (100 μg/mL). After 18−24 h of growth at 37 °C, the cells were collected by centrifugation, resuspended in 20 mL of M63-glucose media (100 μg/mL ampicillin), and grown at 37 °C for 18−24 h. The OD_{600} was determined, and the cells were pelleted and resuspended in lysis buffer (100 mM acetic acid, 1 mM EDTA) at 1 OD unit/mL. The extracts were boiled for 10 min, and cellular debris was removed by centrifugation. The supernatant contained the MccB17 antibiotic and was aliquoted and stored at −80 °C. For the liquid culture bioassay, an overnight culture of a MccB17-sensitive *E. coli* strain, ZK4, was diluted 1:100 into 2 mL of fresh LB. Antibiotic-containing extracts prepared as described above from the mutant or wild-type strains were added (0, 5, 10, 20, 40, 60, and 80 μL). After the cultures were grown at 37 °C for 5 h, the OD_{600} was determined as an indicator of cell growth.

Mass Spectrometric Determination of Heterocycle Content. Reconstituted MccB17 synthetase (4 μM MBP-McbB, 4 μM MBP-McbC, and 1.4 μM McbD) was incubated with the His_6-McbA substrate (20 μM) in synthetase buffer at 37 °C for 30 h. The mixture of unprocessed substrate and heterocyclic products was separated from the synthetase by coelution off a C_{18} RP-HPLC column (solvent A = H_2O + 0.1% TFA; solvent B = CH_3CN + 0.1% TFA; 10−23% B over 25 min). The lyophilized residue was redissolved in

78:20:2 CH_3CN−water−acetic acid for electrospray ionization Fourier transform mass spectrometry, which was performed using a 9.4 T instrument built and maintained at the National High-Field FT-ICR User Facility (*34*). Spectra were analyzed using Isopro v.3.0 software. Reported mass values correspond to the isotopic peak with four heavy isotopes (e.g., $^{13}C_4$).

RESULTS

Overexpression and Purification of MBP-McbB, MBP-McbC, and MBP-McbD. The purification of individual McbB, -C, and -D subunits present in MccB17 synthetase was a prerequisite for the characterization of each protein. We initially attempted to purify McbB, McbC, and McbD without affinity tags. However, this approach proved difficult in the absence of activity assays for the individual proteins required to monitor the purification steps. Furthermore, the levels of McbC and McbD produced in *E. coli* were too low to follow their purification by SDS−PAGE, and the purification scheme for McbB was especially tedious. These difficulties prompted us to investigate affinity chromatography as an efficient route to the large-scale purification of the synthetase subunits.

Overexpression of McbB, McbC, and McbD individually in *E. coli* as fusions to a hexa-histidine (His_6) tag (*35*) met with limited success. Both His_6-McbB and His_6-McbC were produced in *E. coli* but exhibited a propensity to aggregate. His_6-McbD was insoluble and could only be purified from inclusion bodies. While these purifications were useful to provide material for subunit-specific antibody production, they did not facilitate stoichiometric or catalytic studies, and we turned to the expression of each subunit of MccB17 synthetase as a fusion to the highly soluble maltose binding protein (MBP) (*36*), which is readily purified under mild conditions.

Three plasmids, pETMBP-McbB, pETMBP-McbC, and pETMBP-McbD, were constructed for expression of the MBP fusion proteins (Figure 2A). Each construct places the gene of interest in frame to an upstream MBP sequence that is followed by a thrombin cleavage site (Figure 2B), which allows the proteolytic removal of the affinity tag from the purified recombinant proteins. A cleavable MBP tag was desired since its presence could interfere with the subsequent reconstitution of synthetase activity. Thrombin proteolysis results in the liberation of proteins with a Gly-Ser-His tripeptide (McbB, McbC) or a Gly-Ser dipeptide (McbD) appended to the N-terminus. The full-length fusion proteins were purified by affinity chromatography on an amylose column (Figure 3), with typical yields of approximately 20 mg of purified protein/L of culture for MBP-McbB and MBP-McbC. Since MBP-McbD is susceptible to proteolytic degradation during expression in *E. coli*, induction time was limited to 1 h, and approximately 10 mg of MBP-McbD protein/L of culture was obtained at somewhat lower purity than the McbB and McbC fusions.

Identification of Cofactors Required for Heterocyclization. Given the availability of the three subunits, the anticipated complexity of the enzyme-mediated heterocyclizations, and our prior detection of coupled ATP hydrolysis, each of the fusion proteins was analyzed for tightly bound prosthetic groups that could provide clues regarding subunit function.

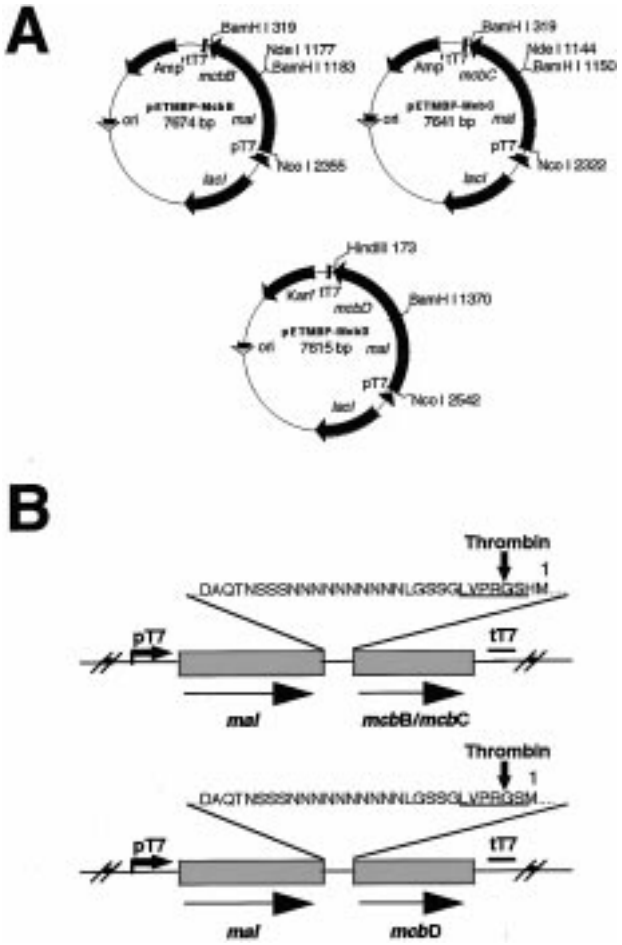

FIGURE 2: Expression vectors for MBP-McbB, MBP-McbC, and MBP-McbD. (A) Plasmid maps of pET-MBP-McbB/C/D. Genes listed include the following: *mcbB/C/D*, genes encoding McbB/C/D, respectively; Amp^r, gene for ampicillin resistance; Kan^r, gene for kanamycin resistance, *mal*, maltose binding protein; *lac*I, lac repressor; pT7, T7 promoter; tT7, T7 terminator. (B) Primary sequences of the linkers connecting the MBP affinity tag to the downstream McbB/C/D proteins. The recognition sites for thrombin are underlined.

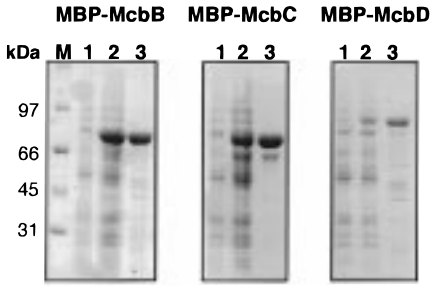

FIGURE 3: Purification of MBP-McbB, MBP-McbC, and MBP-McbD. Proteins were resolved on a 10% SDS−PAGE gel: M = protein markers; lane 1 = cell extract prior to induction with IPTG; lane 2 = cell cultures after 3 h of induction (1 h for MBP-McbD); lane 3 = purified protein.

Analysis of McbB was guided by a limited sequence homology with the zinc binding catalytic site of cytidine deaminase (Figure 4) (Jason Perry, personal communication). The deaminase coordinates zinc at the active site using a single histidine, two cysteines, and a bound water molecule as ligands (*37*), and catalyzes a formally similar deamination/hydration of cytosine nucleosides. McbB contains two such potential zinc binding motifs (site I, residues 133−184, and

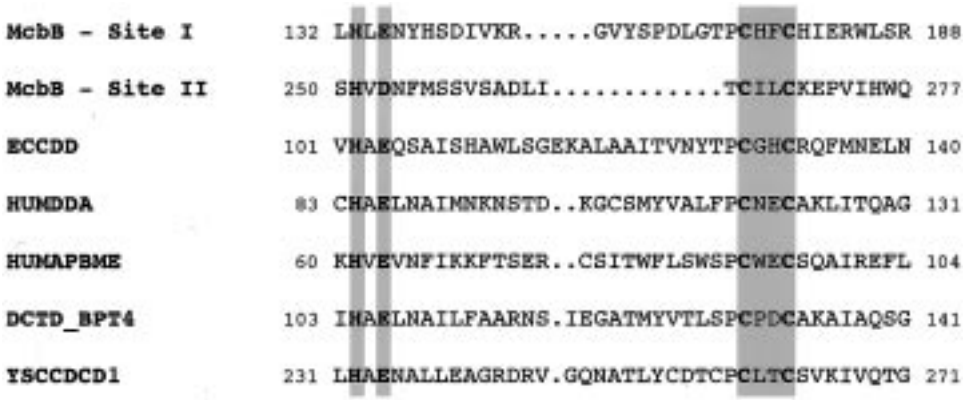

FIGURE 4: Alignment of the putative zinc binding sites in McbB with the catalytic zinc site present in the cytidine deaminase family. Conserved residues are in boldface. The consensus sequence for the cytidine deaminase zinc motif is shaded: ECCDD, *E. coli* cytidine deaminase; HUMDDA, human deoxycytidylate deaminase; HUMAPBME, human apolipoprotein B mRNA editing protein; DCTD_BPT4, T4 deoxycytidylate deaminase; YSCCDCD1, yeast deoxycytidylate deaminase.

Table 1: Zinc Content of Wild-Type and Mutant MBP-McbB Proteins and of MBP-VanX Mutant Proteins Used as Standards[a]

protein	[protein] (μM)[b]	[Zn] (μM)[c]	Zn content (mol %)[d]
WT	98	125	128
C181A/C184A	44	16	37
C266A/C269A	53	30	57
C181A/C184A/C266A/C269A	61	18	30
MBP-VanX (H116A)	173	18	10 (8)[e]
MBP-VanX (D123A)	194	1	0.5 (<0.1)

[a] All proteins were prepared from cells grown in LB media supplemented with 200 μM $ZnSO_4$. [b] Protein concentrations were determined from the corrected absorbance at 280 nm as described in the Experimental Procedures. [c] Protein samples for metal analysis were prepared as described in the Experimental Procedures. The detection limit for inductively coupled plasma atomic absorption spectroscopy was 1 ppb. [d] Percentage values reported for moles of zinc per moles of protein. [e] Numbers in parentheses are published values: McCafferty, D. G., Lessard, I. A. D., and Walsh, C. T. (1997) *Biochemistry 36*, 10498−10505.

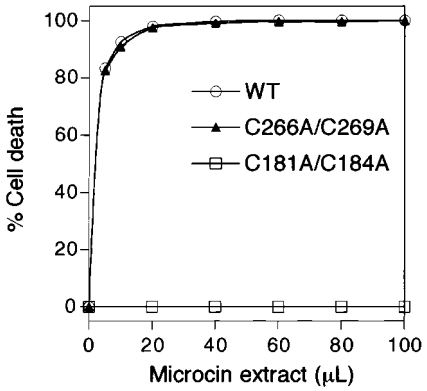

FIGURE 5: Bacteriocidal properties of MccB17. The extent of cell death due to the addition of MccB17 to sensitive cells is plotted against the volume of MccB17 extract added from producing cells containing the wild-type (WT) synthetase or complexes containing mutant Cys → Ala McbB subunits. Mutation of the Cys residues in site I (C181A/C184A) leads to the loss of mature antibiotic production and unaffected growth of sensitive cells. The site II mutations (C266A/C269A) do not perturb microcin production as reflected by the growth inhibition of sensitive cells.

site II, residues 251−269). Metal analysis of wild-type MBP-McbB repeatedly confirmed the presence of zinc (Table 1). McbB contains approximately 1 atom of zinc per protein, although the ICP-AAS data exhibit unusual variability (71−128% zinc content for wild-type MBP-McbB from four different preparations) under conditions where mutants of MBP-VanX, a zinc-containing D-Ala-D-Ala dipeptidase (*31*), gave the anticipated stoichiometric levels.

In these initial studies, we have analyzed how mutation of the pairs of cysteines in sites I and II of McbB affect zinc content. Replacement of both Cys residues at site I with Ala ($McbB_{(C181A/C184A)}$) led to loss of activity in reconstitution assays (vide infra) and complete disruption of antibiotic production as revealed in a bioassay that measures the effect of MccB17 production on the growth of sensitive cells (Figure 5). A 70% reduction in Zn content of the MBP fusion compared to native MBP-McbB was also observed. Conversely, Cys substitutions at site II (MBP-$McbB_{(C266A/C269A)}$) had no effect on the production of mature MccB17 (Figure 5). These mutations did affect the zinc content, albeit to a lesser extent (45% residual). Furthermore, the quadruple mutant, MBP-$McbB_{(C181A/C184A/C266A/C269A)}$, in which all four conserved Cys residues are replaced by Ala, still retained 23% of zinc compared to the native fusion protein. The accuracy and reproducibility of our metal analyses have been confirmed with other metalloproteins of defined zinc content (Table 1).

Purification of MBP-McbC revealed it to be a yellow protein, indicating the presence of tightly bound flavin coenzyme. An optical spectrum of the protein (Figure 6A) confirmed the presence of stoichiometric quantities of flavin, identified as FMN by HPLC analysis (Figure 6B). This makes McbC the likely candidate for mediating the redox step that occurs in each ring-forming catalytic cycle as the thiazoline and oxazoline intermediates are desaturated to the corresponding thiazoles and oxazoles. The resulting dihydroflavin needs to be reoxidized for cofactor recycling to occur. Molecular O_2 serves this purpose in vitro, although other terminal electron acceptors are probably involved in vivo since MccB17 production can occur anaerobically (data not shown).

Recent studies on the McbD subunit of MccB17 synthetase have shown that this protein may function as a regulated ATPase/GTPase (*28*). Although this coupled, substrate-dependent activity is observed when McbD comprises part of the synthetase complex, the purified McbD subunit alone showed no ability to hydrolyze ATP. Development of a

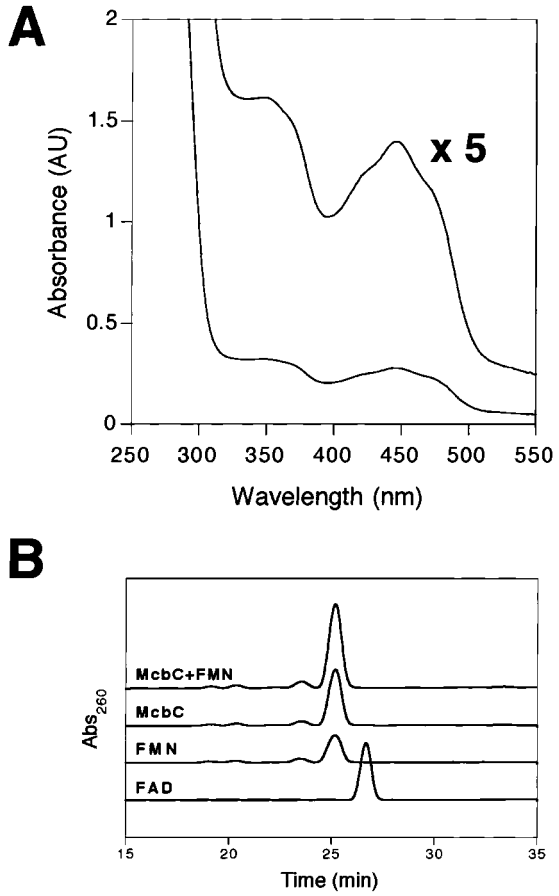

FIGURE 6: McbC contains FMN. (A) UV−Vis spectrum of purified MBP-McbC showing absorbances characteristic of a flavin cofactor (λ_{max} = 348 and 446 nm). The spectrum was collected in 50 mM HEPES, pH 8.0. (B) HPLC analysis of the flavin released from MBP-McbC.

reconstitution assay would hence facilitate analysis of this activity in vitro.

Photolabeling of the MccB17 Synthetase Complex. We have previously reported that the McbA propeptide (residues 1−26), essential for detection of any substrate turnover, functions as a weakly amphipathic α-helix, which recruits the McbB, -C, -D synthetase complex for effecting post-translational heterocyclization (*29*). In particular, alanine scanning mutagenesis revealed a hydrophobic surface in the propeptide comprised of residues Phe[8] and Leu[12] that was critical for synthetase recognition. Since the 26-residue propeptide alone is a potent inhibitor of the synthetase, with a K_i (2 μM) essentially equivalent to the K_M of substrate (2.3 μM) (*23*), a synthetic propeptide analogue (biotinyl-F8BPA) with Phe[8] substituted by L-4-benzoylphenylalanine was prepared and utilized in a photolabeling experiment to identify the propeptide recognition subunit within the native synthetase complex. A biotin moiety was appended to the N-terminus of this synthetic propeptide to facilitate detection after any photoinduced cross-linking by conventional avidin-based techniques.

Synthetase activity was monitored by western immunoblots probed with anti-MccB17 antibodies that specifically recognize the heterocyclic (oxazole/thiazole-containing) products (*19*). Competitive inhibition assays at 20 μM substrate (MBP-McbA) demonstrated that the biotinyl-F8BPA 26-mer inhibited the CBP-tagged synthetase complex with detectable

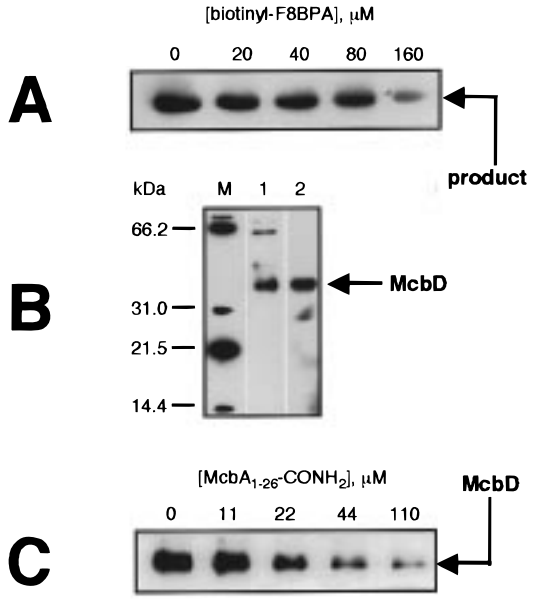

FIGURE 7: Photolabeling of McbD. (A) Western immunoblot assay probed with anti-MccB17 antibodies for the activity of native MccB17 synthetase, showing the competitive inhibition of substrate turnover (20 μM MBP-McbA) by increasing concentrations (0−160 μM) of the biotinyl-F8BPA propeptide analogue. (B) Western blot analysis of the photolabeling experiment (see text for details), probed with HRP-conjugated avidin (lane 1) and anti-McbD antibodies (lane 2). The McbD subunit in the synthetase complex is exclusively labeled by the biotinyl-F8BPA photolabel: M = biotinylated molecular mass markers. (C) Western blot analysis probed with HRP-avidin, demonstrating substrate protection by increasing concentrations (0−110 μM) of synthetic propeptide ($McbA_{1-26}$-$CONH_2$) in the photolabeling of McbD by biotinyl-F8BPA (12.5 μM).

affinity (IC_{50} ~60 μM, Figure 7A), setting the stage for subsequent photolabeling experiments. Biotinyl-F8BPA was incubated with the native synthetase complex for 1 h and irradiated with UV−vis light (λ = 350 nm). The McbB (33 kDa), McbC (31 kDa), and McbD (43 kDa) subunits were resolved by SDS−PAGE, and biotinyl-F8BPA-labeled subunits were detected by western blots probed with HRP-conjugated avidin. As illustrated in Figure 7B, a 43 kDa protein was labeled by BPA-$McbA_{1-26}$ (lane 1). Western immunoblots of the reaction mixture performed in parallel and probed with anti-McbB, anti-McbC, and anti-McbD antibodies confirmed that this protein was McbD (Figure 7B, lane 2). Protection experiments were subsequently performed to verify the specificity of the photolabel. The addition of a 9-fold excess of synthetic propeptide ($McbA_{1-26}$-$CONH_2$) was observed to virtually eliminate photolabeling of the McbD subunit by biotinyl-F8BPA (Figure 7C), confirming that this subunit contains the propeptide recognition site. Additional photolabeling experiments have revealed that purified McbD does not bind the biotinyl-F8BPA propeptide in the absence of the other subunits (data not shown), emphasizing the importance of subunit association for substrate recognition and turnover.

Reconstitution of MccB17 Synthetase in Vitro. The ability to purify individual subunits of MccB17 synthetase enabled attempts at reconstitution of heterocyclization activity. Initially, the three full-length MBP-McbB, -C, and -D fusion proteins were combined together in stoichiometric ratios and incubated with PNP-$McbA_{1-46}$. This substrate incorporates the first bisheterocyclization site of McbA. Aliquots of the

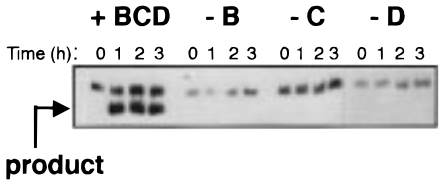

FIGURE 8: Reconstitution of MccB17 synthetase monitored by western immunoblots probed with anti-MccB17 antibodies. Incubation of the synthetic PNP-McbA$_{1-46}$ substrate (20 μM) with all three subunits (4 μM each thrombin-clipped subunit, + BCD) leads to heterocyclic product formation, whereas pairwise combinations of the subunits (-B, -C, -D) are inactive. The higher molecular weight band present in each lane arises from nonspecific recognition of a contaminant by the polyclonal antibodies.

reconstitution mixture were analyzed for heterocycle formation at appropriate time points using the western immunoblot assay described earlier. Although the polyclonal anti-MccB17 antibodies used in this assay can detect even a single heterocycle (out of the eight produced in mature MccB17), no product formation was observed under conditions wherein 0.01% of the specific activity of the native synthetase complex could have been easily detected. Next, the MBP tag was removed from each fusion protein by digestion with thrombin (0.03 units of protease, 1.6 nmol of fusion protein, 25 °C, 2 h), and the reconstitution experiment was repeated. As shown in Figure 8, time-dependent formation of the 4,2-fused oxazole-thiazole was only observed when all three thrombin-clipped subunits were combined (4 μM each subunit, 20 μM PNP-McbA$_{1-46}$). In contrast, pairwise combinations of McbC and McbD (Figure 8, "-B"), McbB and McbD ("-C"), or McbB and McbC ("-D") did not result in reconstitution of synthetase activity, demonstrating that all three subunits of MccB17 synthetase are necessary and sufficient in catalyzing oxazole and thiazole formation.

Optimizing the Yield of Reconstituted Complex. The ability to reconstitute heterocyclization activity only after thrombin digestion of the subunits indicated that the affinity tag on one or more of the McbB, -C, and -D proteins was interfering with complex formation. To identify the subunits that were inactivated by fusion with MBP, we attempted four reconstitutions in parallel. Each of the subunits was treated with thrombin in the control experiment, whereas the other three assays involved pairwise combinations of digested subunits, with the remaining component being added as the full-length MBP fusion protein. Benzamidine, a potent inhibitor of thrombin, was added to these assays (2 mM final concentration) to prevent inadvertent digestion of the subunit retained as the MBP fusion. As shown in Figure 9, MBP-McbB and MBP-McbC function almost as well as the cleaved proteins. In contrast, the intact MBP-McbD fusion protein is virtually inactive in the reconstitution assay.

The above results prompted us to examine the thrombin digestion conditions more closely. Briefly, 200 pmol of each MBP fusion protein was incubated at room temperature with increasing amounts of thrombin. After 15 min, the digestion was quenched with benzamidine, a portion of each digest was prepared for SDS−PAGE analysis to determine the extent of digestion, and the rest was used in a reconstitution assay with GGC as substrate, as described earlier. As shown in Figure 10A, the digests did not proceed to completion. Instead, the yields of released subunit were 30% for McbB, 82% for McbC, and 68% for McbD. Longer incubations with

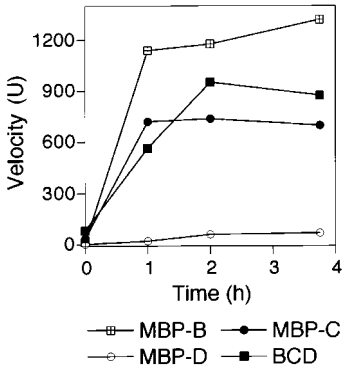

FIGURE 9: MBP-McbB and MBP-McbC are active as fusion proteins. Kinetics of product formation were obtained by western immunoblot analysis of assays run in parallel as described in the Experimental Procedures. Reconstitution was attempted using subunits (4 μM each) as follows: all cleaved from the MBP tags ("BCD"), MBP-McbB + cleaved McbC/D ("MBP-B"), MBP-McbC + cleaved McbB/D ("MBP-McbC"), and MBP-McbD + cleaved McbB/C ("MBP-McbD"). MBP-McbD is virtually inactive in reconstitution activity. PNP-McbA$_{1-46}$ (20 μM) was used as substrate.

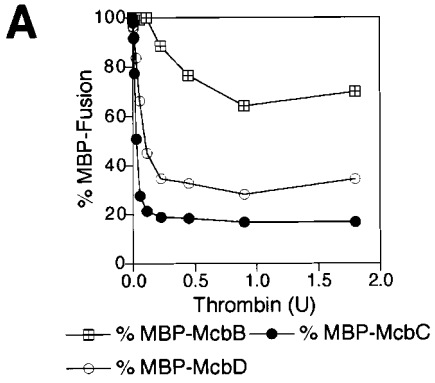

FIGURE 10: Thrombin titration data for the digestion of MBP-McbB, MBP-McbC, and MBP-McbD. (A) Extent of thrombin proteolysis for each MBP fusion protein after a 15 min digest at room temperature, monitored by SDS−PAGE. (B) Activity of the digested subunits, measured by western immunoblot after incubation of the corresponding reconstituted synthetases with the GGC substrate for 1 h at 37 °C.

higher thrombin−protein ratios did not improve the cleavage efficiencies (data not shown), implying that the thrombin sites were not readily accessible (as might be expected if there was a population that included some misfolded fusion proteins).

The western immunoblot data for product formation confirm that MBP-McbB and MBP-McbC can reconstitute synthetase complex and illustrate the significant increase in reconstitution activity (from 150 to 600 activity units in the

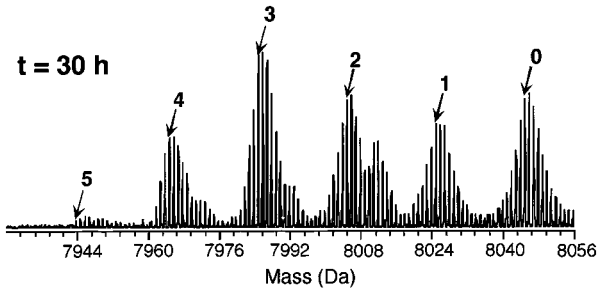

FIGURE 11: Partial EFI/FTMS mass spectrum of the reaction products obtained after incubation of the His_6-McbA substrate with the reconstituted MccB17 synthetase for 30 h. Discrete heterocyclic products containing 1−5 heterocycles (corresponding to a mass decrease of 20−100 Da, respectively) are observed; arrows indicate the fourth heavy isotope peak for each species. Scale is set to mass.

immunoblot assay) as McbD is released from the corresponding MBP fusion protein (Figure 10B). The data also indicate an optimum level of thrombin to be used in subsequent reconstitutions (0.056 units), since the activities of both McbC and McbD decrease at high levels of protease. As illustrated in Figure 10B, McbD was the most sensitive subunit; it became completely inactivated at higher protease concentrations (data not shown). Since no high-affinity thrombin sites are present in McbC or McbD, this inactivation probably results from nonspecific cleavage of the proteins at high protease concentrations.

On the basis of the results from the thrombin digests, the assay protocols were modified so that MBP-McbD alone was treated with thrombin prior to reconstitution with MBP-McbB and MBP-McbC. This strategy reduces some of the heterogeneity in complex formation that would result in a mixture of partially digested MBP-McbB and -C proteins, each of which competes with the corresponding cleaved subunit in the reconstitution process. Treatment of MBP-McbD with the specified units of thrombin maximizes the activity realized from the cleaved subunit, even though only 34% of the fusion protein is released under these conditions.

Specific Activity of the Reconstituted Synthetase. Western immunoblot assays with GGC as substrate revealed that the specific activity of the reconstituted MccB17 synthetase was approximately 100-fold lower than that of CBP-tagged MccB17 synthetase or the wild-type complex (data not shown). This result was supported by mass spectrometric analysis of the heterocyclization of His_6-McbA after a 30 h incubation with the reconstituted synthetase (Figure 11). For each oxazole or thiazole formed, a loss of 20.03 Da is expected (loss of water and two hydrogens). A mass value of 8043.74 Da for the unmodified substrate (Figure 11, isotopic cluster at far right) was within experimental error of the predicted value (8043.68 Da). Isotopic distributions resulting from the loss of multiples of 20.02 ± 0.03 Da were also observed, corresponding to discrete products containing 1, 2, 3, 4, and 5 heterocycles (denoted by arrows in Figure 11). These results indicated that the reconstituted enzyme modified substrate distributively, as has been observed in the bisheterocyclization of $McbA_{1-46}$ by the native synthetase (*26*). However, only five of the eight heterocycles were processed in 30 h, and a large fraction of the substrate remained unmodified. In a separate study, near complete heterocyclization of His_6-McbA was obtained with the native synthetase in only 16 h (N. L. Kelleher and C. T. Walsh, manuscript in preparation).

The lower specific activity of the reconstituted synthetase was not unexpected, since prior observations (limited solubility of the purified subunits, variable metal analyses of McbB, and incomplete thrombin digestions) had suggested that populations of each protein might contain misfolded conformers. In this regard, complex formation probably contributes to the stabilization of each subunit in vivo. Nevertheless, the sensitivity of the western immunoblot and mass spectrometry assays is more than sufficient for practical applications of the reconstituted synthetase in probing the formation of oxazoles and thiazoles in vitro.

Titration of each McbB, -C, and -D Subunit into the Reconstituted Synthetase Complex. The copurification of McbB, -C, and -D as a multimeric MccB17 synthetase complex in both standard and affinity-based purification strategies suggested that the subunits were closely associated with each other. To estimate the magnitude of intersubunit interactions, we used reconstituted activity to monitor subunit titrations. Two subunits were maintained at a fixed concentration (4 μM), while the third subunit was added in increasing amounts (0−8 μM). An exception was the titration of McbD, the maximum effective concentration of which was limited to 2.7 μM because the thrombin digest of the relatively insoluble MBP fusion released only 34% of the active protein.

The activity curve of each subunit titration exhibits saturation kinetics (Figure 12), and was used to calculate the stability of the reconstituted complex. The apparent dissociation constant ($K_{D,app}$) for McbD is 1.7 ± 0.6 μM. We cannot calculate a $K_{D,app}$ for either the MBP-McbB or the MBP-McbC subunit, because McbD could not be maintained at saturating concentrations ([McbD] = 1.4 μM in these assays). However, we can report a $K_{complex}$ defined as the subunit concentration at which 50% of reconstituted activity is observed ($K_{complex,MBP-McbB} = 1.0 \pm 0.1$ μM; $K_{complex,MBP-McbC} = 1.8 \pm 0.8$ μM). The three subunits therefore exhibit at least micromolar affinities for each other. The subunit affinities may even lie in the nanomolar range, since the low specific activity of the reconstituted synthetase indicates that only a small percent of the subunits actually reconstitutes into active complex.

Although the data presented thus far suggest an intimate association of the McbB, -C, and -D proteins in a single complex that catalyzes oxazole and thiazole formation, it was unclear as to whether certain subunits could function in isolation and produce intermediates for further processing by the other proteins. To investigate this possibility, the MBP-McbB, MBP-McbC, and McbD proteins (individually and in pairwise combinations) were incubated with substrate ($PNP\text{-}McbA_{1-46}$) for 1 h. The subunits were subsequently removed by ultrafiltration through a Microcon-10 filter unit (MWCO = 10 kDa), which only allows the passage of substrate (4332 Da) and any potential intermediates or product. The filtrate was then incubated with the remaining subunit(s), and heterocycle formation was assessed by western immunoblots. To ensure that hydrophobic intermediates or products were not irreversibly bound to the ultrafiltration membrane, CBP-tagged MccB17 synthetase was incubated with $PNP\text{-}McbA_{1-46}$ under the same conditions and the assay mixture was applied to a Microcon-10 filter unit prior to western immunoblot analysis. Heterocyclic product was detected only in this control experiment and

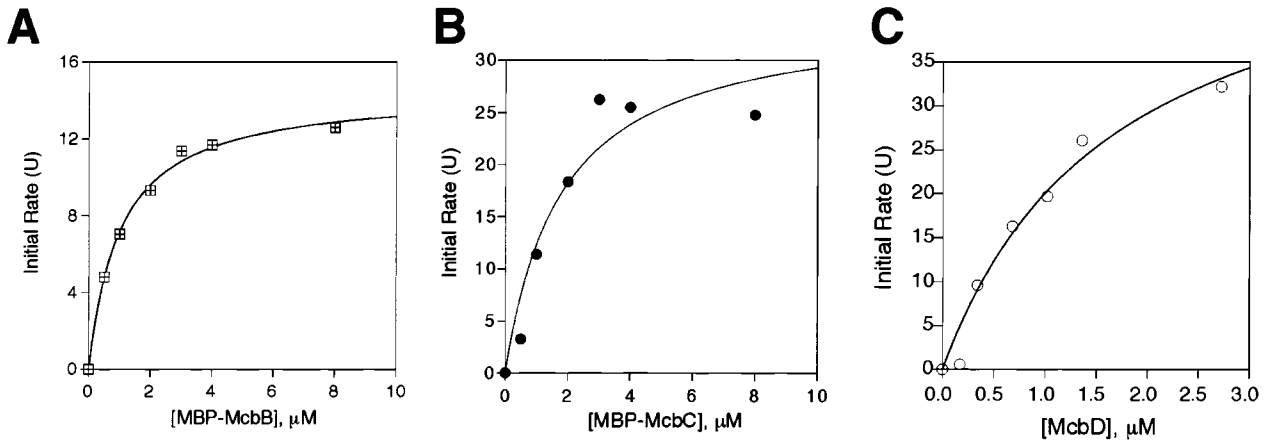

FIGURE 12: Titration of MBP-McbB, MBP-McbC, and McbD subunits in the reconstitution assays. Assays were conducted at 37 °C, and the concentrations of the remaining two subunits were maintained at 4 μM (1.4 μM for McbD). The initial rates of product formation at each subunit concentration were measured over a period of 12 min by western immunoblots run in duplicate. The effective concentration of McbD was relatively low due to poor solubility and incomplete thrombin proteolysis of the fusion protein. Each titration curve exhibits saturation kinetics and reflects micromolar affinities in complex formation. See text for details.

not in the other incubations (data not shown). With the proviso that the release of extremely short-lived intermediates might have escaped detection, these results confirm that all three subunits are required to function in concert for the turnover of the McbA substrate.

Reconstitution Analysis of Mutant Subunits. Since the reconstitution incubations can be made limiting in any of the three components MBP-McbB, MBP-McbC, or McbD during activity assays (Figure 12), the ability of mutant proteins to substitute for wild-type McbB, -C, or -D can be assessed. In particular, an initial sorting between catalytically inactive but complex-competent mutants (dominant negative) and inactive, complex-incompetent mutants is enabled by such reconstitution assays. As shown in Figure 13A, the MBP-McbB$_{C181A/C184A}$ double mutant described earlier competitively inhibits reconstitution by wild-type MBP-McbB ($IC_{50} = 4$ μM) in titration experiments using 4 μM each of MBP-McbB/MBP-McbC and 1.4 μM McbD. Under these conditions, 80% inhibition was obtained with a 10-fold excess of MBP-McbB$_{C181A/C184A}$, suggesting that these mutations inhibit catalytic function but not partner protein recognition during complex formation. In contrast, an McbD$_{D147A}$ mutant subunit (prepared by thrombin proteolysis of the corresponding MBP fusion protein) was not an inhibitor of reconstitution, even when present in 7.5-fold excess over wild-type McbD (Figure 13B), and hence falls in the second category, where the mutation affects complex assembly. In accord with this result, when McbD$_{D147A}$ was expressed in tandem with McbC and CBP-tagged McbB, we were unable to copurify a multimeric mutant synthetase (*28*).

Lack of Requirement for HtpG in Reconstitution of MccB17 Synthetase. In purifications of wild-type MccB17 synthetase (*23*), four proteins were observed to copurify with oxazole/thiazole-forming activity: McbB, -C, -D, and HtpG, the latter being an *E. coli* member of the Hsp90 family of heat shock proteins (*38*). In fact, HtpG was the most abundant protein component in the preparations of purified synthetase. On the other hand, HtpG does not copurify with CBP-tagged MccB17 synthetase, and its absence does not adversely affect the activity of the affinity-purified complex relative to wild-type synthetase (*25*). Nevertheless, the low levels of activity observed here with reconstituted MccB17 synthetase prompted

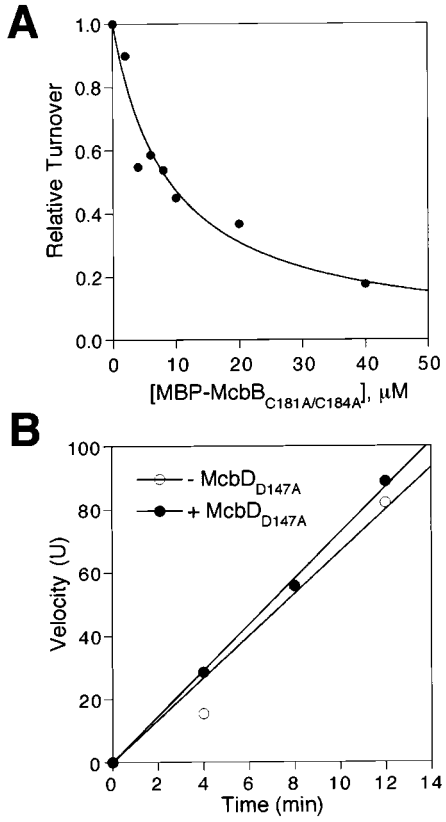

FIGURE 13: MBP-McbB$_{C181A/C184A}$ is a competitive inhibitor of reconstitution by wild-type MBP-McbB. MBP-McbD$_{D147A}$ does not participate in reconstitution. (A) Increasing concentrations of MBP-McbB$_{C181A/C184A}$ were titrated into a reconstitution mixture containing 4 μM MBP-McbB/C and 1.4 μM McbD. The initial rates of turnover of GGC (20 μM) were measured over a 12 min period at each concentration of mutant subunit, using western immunoblots run in duplicate. (B) Kinetics of product formation for a reconstitution assay in the presence of a 7.5-fold excess of McbD$_{D147A}$ (10.2 μM, "+ McbD$_{D147A}$") relative to the control (0 μM, "− McbD$_{D147A}$"). The concentrations of MBP-McbB/C, McbD, and GGC were the same as in part A. The rates are identical in both assays, indicating that McbD$_{D147A}$ does not compete with McbD for complex formation.

us to assess whether HtpG could influence the net yield of active synthetase by functioning as a positive effector of complex assembly. Both in vivo bioassays of MccB17

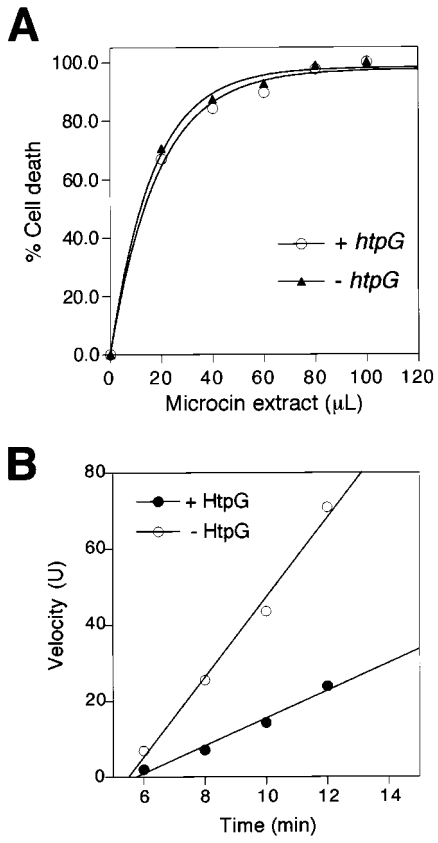

FIGURE 14: Effect of HtpG on MccB17 antibiotic production. (A) Bioassay data reflecting the growth inhibition of MccB17-sensitive *E. coli* ZK4 cells exposed to extracts of antibiotic producing cells that contain (+ *htpG*) or lack (− *htpG*) a functional *htpG* gene. (B) Effect of HtpG on reconstitution of MccB17 synthetase in vitro. Reconstitution assays were performed as described in the Experimental Section, in the absence of affinity-purified His_6-HtpG ("− HtpG"), and in the presence of a 10-fold excess of His_6-HtpG (40 μM, "+ HtpG"). The presence of the chaperone leads to a 3-fold decrease in reconstitution activity.

antibiotic production and in vitro reconstitution experiments were therefore compared in the presence and absence of this chaperone.

When MccB17 antibiotic production by *E. coli* strain MC4100Δ*htpG* deleted for *htp*G (*23*) was compared to that of the parental strain (Figure 14A), there was no effect on MccB17 production in vivo, implying that the copurification of HtpG with MccB17 synthetase was potentially an artifact, or that another *E. coli* chaperone could substitute for HtpG. To examine the effect of HtpG on the reconstitution of MccB17 synthetase in vitro, we expressed the chaperone as a fusion to a hexahistidine (His_6) tag and purified it by Ni^{2+} chelate chromatography. His_6-HtpG has been shown to retain ATPase activity in vitro (*39*), suggesting that its chaperone function is not impaired. However, instead of stimulating activity, the addition of a 10-fold excess of His_6-HtpG (40 μM) to the reconstitution assay unexpectedly *reduced* heterocyclic product formation 3-fold (Figure 14B). Since the reconstitution process is insensitive to high concentrations of other proteins (e.g., BSA) and ATP was in excess (2 mM), this drop in activity is probably due to the sequestration of one or more subunits by the chaperone. Hence, the role of HtpG in MccB17 synthetase assembly or activity remains unclear, although the protein clearly does not chaperone the McbA substrate to the multimeric synthetase complex. As the native function of HtpG in *E. coli* is still unknown, we can only speculate that this chaperone mediates complex assembly or stabilizes protein subunits prior to the hetero-oligomerization.

DISCUSSION

This work describes the purification and characterization of the three subunits of the *E. coli* enzyme complex MccB17 synthetase, which catalyses peptide-derived heterocyclization. This post-translational modification catalyst introduces 8 five-membered rings (4 thiazoles and 4 oxazoles) in the maturation of the 69 aa McbA preproantibiotic as it operates on 14 of the last 43 residues of substrate. Since thiazole- and oxazole-containing peptides exhibit a diverse range of therapeutic activities, and the 4,2 tandemly connected bis-heterocycles in particular (e.g., in microcin B17, bleomycin, and thiostrepton) are likely to target nucleic acids (*3*, *4*, *40*, *41*), dissection of the enzymatic logic of their post-translational biosynthesis may be useful as well as mechanistically valuable.

In initial studies, crude extracts from cultures of single subunit knockouts (i.e., $McbB^-$, $McbC^-$, $McbD^-$) were added to extracts containing the complementing wild-type subunit. However, no activity was reconstitutable in any configuration of mixing (*23*), suggesting a pronounced in vivo lability of isolated subunits and/or incomplete, inactive synthetase complexes. To purify the three presumed catalytic McbB, -C, -D subunits under mild conditions suitable for reconstitution, we attempted both His_6-tagged and MBP fusion strategies. The His_6-tagged proteins were poorly soluble, aggregated, and produced no reconstitutable heterocyclization activity. The N-terminal MBP fusions had the advantages of good expression, increased solubility, and rapid purification under conditions where metals would not be stripped from the parent proteins. However, the large (~43 kDa) MBP domain was anticipated to block reassembly of one or more of the McbB, -C, or -D subunits. In fact, no heterocyclization activity was detectable when all three purified MBP fusion proteins were mixed. Nevertheless, thrombin cleavage of the affinity tags has afforded some initial success in synthetase reconstitution. Indeed, two of the components (McbB and McbC) can tolerate the N-terminal MBP domain without deleterious effects, although McbD cannot reassemble until cleaved away from the affinity tag. The reconstitution of activity, assessed by immunoblots with antibody that can detect a single heterocycle, and by mass spectrometry (loss of 20 Da per ring introduced) is modest to date, but nonetheless extremely useful and promising.

Three clear utilities of the reconstitution assay have been described. First, it establishes that all three subunits are required and must be present together for substrate turnover: there are no diffusable intermediates produced in the absence of any one of the subunits. Second, the cofactor content of isolated subunits can be related to function. Third, mutations in specific subunits can be evaluated for their effects on complex assembly. This attribute in particular will permit evaluation of subunit-specific function and classification of mutations depending on the extent to which they perturb interactions with other subunits. For example, the mutant $McbD_{D147A}$ subunit is unable to compete with wild-

Scheme 1

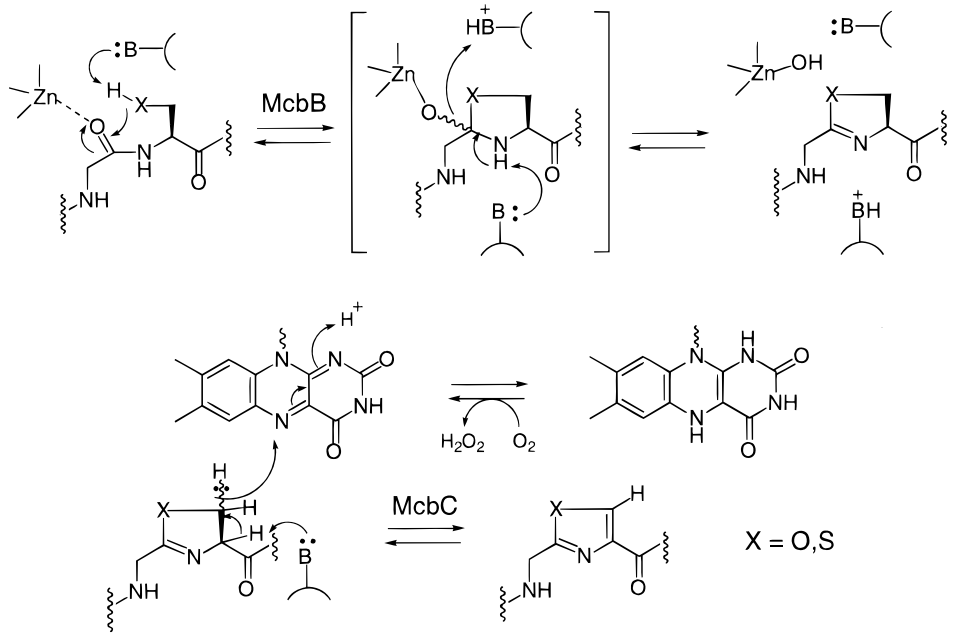

type McbD, and most likely possesses an altered architecture. In contrast, the McbB double Cys→Ala mutant (MBP-$McbB_{C181A/C184A}$) acts as a dominant negative, suggesting that the lack of activity may have a catalytic explanation. Prospectively, mutants in the McbC flavoprotein component may be of particular interest to be categorized in such reconstitution assays, as they may allow the isolation of oxazoline/thiazoline-containing intermediates. The tasks of optimizing yields and of purifying reconstituted active complex away from unincorporated subunits to determine parameters such as stoichiometry and catalytic turnover numbers also lie ahead, as does establishing the role of endogenous chaperones such as HtpG in complex assembly or maintenance.

The detection of zinc in isolated, reconstitutable MBP-McbB and of FMN in MBP-McbC (both in stoichiometric quantities) provides a better mechanistic platform for analysis of the sequential transformations that MccB17 synthetase is presumed to perform in each of its eight catalytic cycles during maturation of the active antibiotic (Scheme 1). Starting from the chemically reasonable assumption that cyclodehydration to oxazolines and thiazolines precedes dehydrogenation (and the experimental result that no M-2 dehydro intermediates are detected by mass spectrometry (*26*)), the initial step in each catalytic cycle is the cyclization of the Ser or Cys side chain on the amide carbonyl of the upstream glycine residue. General base catalysis is expected to generate the alkoxide or thiolate nucleophile, respectively (Scheme 1), for this step. The resulting tetrahedral adduct (aminal or thiohemiaminal) needs to be regioselectively protonated to control the routes of decomposition. For example, protonation of the tetrahedral oxyanion facilitates dehydration to oxazoline/thiazoline, whereas protonation of the erstwhile amide nitrogen would labilize the C−N bond for cleavage along the pathway followed by such autocleaving proteins as the inteins (*42*), the hedgehog family (*43*), and amino-terminal nucleophile aminohydrolases such as the proteasome β-subunit (*44*).

Scheme 2

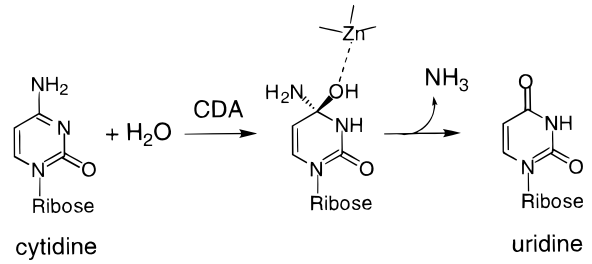

Several enzymes that catalyze reversible dehydrations are zinc-containing proteins (*45*). In particular, the cytidine and adenine deaminases have some mechanistic analogy to the dehydrations in microcin B17 dihydroheterocycle formation in that addition of H_2O into an imine double bond to yield the sp^3 center at C_4 (Scheme 2), when viewed in the reverse direction, is the same reaction as that postulated above for oxazoline and thiazoline formation. The X-ray structure of *E. coli* cytidine deaminase (CDA) reveals zinc in the active site coordinated via His^{102}, Cys^{129}, and Cys^{132} (*37*). Glu^{104} serves as the catalytic base for activation of the water molecule coordinated as the fourth ligand to zinc (*46*). Our finding that McbB contains zinc raises the likelihood that it is the dehydration catalyst. The initial Cys mutations reported herein indicate the $Cys^{181,184}$ pair as more important to antibiotic production than the $Cys^{266,269}$ pair (Figure 5), but the zinc content is not completely abolished in the mutants. It is possible that each McbB protein contains two zinc ions (one catalytic, and the other structural), and this proposal will be investigated in future studies. By association with its dehydration activity, McbB is also likely to be the cyclase, that is, a cyclase/dehydrase. There are few precedents for such zinc cyclases, but the zinc-dependent dihydroorotase (DHOase) (*47*), which converts *N*-carbamoylaspartate to cyclic dihydroorotate, may have some mechanistic analogy.

Once thiazoline and oxazoline rings are formed in the active site of the heterotrimeric MccB17 synthetase, they apparently do not get released nor do they accumulate before

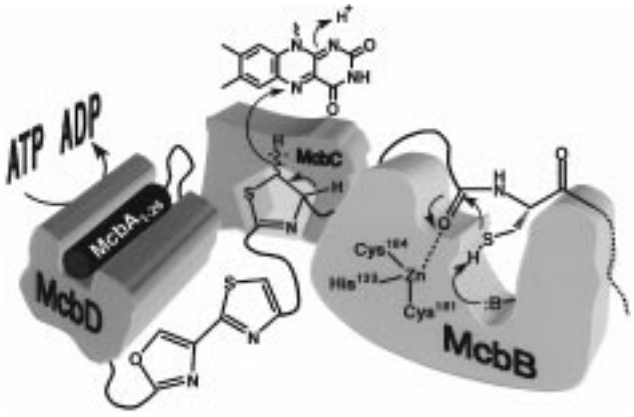

FIGURE 15: Proposed model for the activity of MccB17 synthetase. The McbD subunit (left) contains a site that binds the helical propeptide sequence ($McbA_{1-26}$), which is the prime recognition determinant for the McbA substrate. A polyglycine linker (not shown) sets the register that aligns downstream heterocyclizable Ser and Cys residues with the active site comprising the McbB and McbC proteins. McbB (at right) may function as a zinc-dependent cyclodehydratase and facilitate the cyclization of Ser and Cys side chains at the upstream peptide carbonyls. The resulting tetrahedral transition states are dehydrated to form the corresponding oxazolines and thiazolines, which are further desaturated by the McbC flavoenzyme (center), which functions as a dehydrogenase. The substrate-dependent hydrolysis of ATP to ADP by McbD may function as a conformational switch (not shown) that facilitates the heterocyclization process, or serve a motor function in the distributive formation of all eight heterocycles, which are dispersed over a stretch of 30 residues in McbA.

Scheme 3

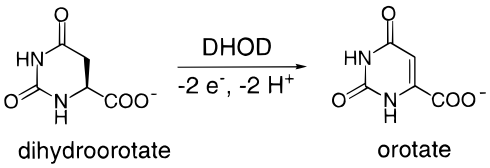

undergoing C_4-C_5 desaturation (no M-18 dihydro intermediates are detected by mass spectrometry (*26*)). The desaturation bears formal analogy to another enzymatic step in pyrimidine metabolism, the olefin-forming conversion of dihydroorotate to orotate (Scheme 3), catalyzed by dihydroorotate dehydrogenase (DHOD) (*48*). DHOD is a flavoprotein desaturase, most likely mediating olefin generation by proton/hydride transfer to yield oxidized heteroaromatic product and E-$FMNH_2$. It is likely that McbC, also an FMN enzyme from this study, is the cognate olefin-forming desaturase in the eight catalytic cycles of MccB17 synthetase (Figure 15). In each case, the E-$FMNH_2$ must be reoxidized by an electron acceptor (O_2, an iron−sulfur protein, or an electron-transfer flavoprotein).

If McbB and McbC act to carry out the catalytic steps as suggested in Scheme 1 and Figure 15, what then of McbD? We have described a substrate-coupled conditional ATPase/GTPase activity of MccB17 synthetase (stoichiometry of 5 ATP cleaved per heterocycle formed under a specific set of conditions) (*28*) and have noted signature motifs in McbD reminiscent of the ATP and GTP binding domains of GTPases. It is likely that McbD is the ATPase/GTPase (Figure 15), but the isolated subunit does not show this activity, even in the presence of McbA. This activity may therefore be a tightly regulated property of the complex and could be used to alter conformations of effector domains that govern interaction with the McbB and McbC subunits, consistent with the observed failure of the $McbD_{D147A}$ mutant to assemble. Intriguingly, Asp^{147} is part of a DXXG consensus sequence within the potential ATPase domain of McbD (*28*), which has been implicated in conformational changes between GTP- and GDP-bound forms in the G protein family (*49*). A second feature of note in MccB17 synthetase is its so far absolute requirement for the 26 aa propeptide region of McbA in substrate recognition, binding, and catalysis (*24*, *29*). Using a biotinylated-benzoylphenylalanine analogue of $McbA_{1-26}$, we have now detected selective cross-linking of the specificity conferring propeptide to McbD in a manner protected by substrate (but independent of ATP). This observation suggests that McbD is the subunit that recognizes the amphipathic α-helical propeptide as depicted in Figure 15. In vivo, it is likely that the McbB, -C, -D trimer is in an E−S complex with McbA at the cytoplasmic membrane, poised to secrete mature microcin through the McbE/F ATPase pump.

The ability to purify the separate McbB, −C, −D subunits in wild-type and mutant forms as MBP fusions, and the successful demonstration of reconstitution of heterocyclization activity, even at the low levels achieved to date, sets up approaches to analyze further the molecular logic of post-translational modifications of peptide substrates to conformationally constrained heterocycles, including tandem arrays that target DNA, RNA, and the protein synthesis machinery in cells.

ACKNOWLEDGMENT

We thank Jason Perry for useful discussions and Dr. Florian Hollfelder for critical reading of the manuscript. We also thank Alan Marshall for maintaining and granting access to the 9.4 T ESI/FTMS mass spectrometer (National High-Field FT-ICR MS Facility, NHMFL, NSF CHE-94-13008).

REFERENCES

1. Sinha Roy, R., Gehring, A. M., Milne, J. C., Belshaw, P. J., and Walsh, C. T. (1999) *Nat. Prod. Rep.* (in press).
2. Takita, T., Muraoka, Y., Nakatani, T., Fujii, A., Umezawa, Y., and Naganawa, H. (1978) *J. Antibiot. 31*, 801−804.
3. Vanderwall, D. E., Lui, S. M., Wu, W., Turner, C. J., Kozarich, J. W., and Stubbe, J. (1997) *Chem. Biol. 4*, 373−387.
4. Zuber, G., Quada, J. C., Jr.,and Hecht, S. M. (1998) *J. Am. Chem. Soc. 120*, 9368−9369.
5. Ressler, C., and Kashelikar, D. K. (1968) *J. Am. Chem. Soc. 88*, 2025−2035.
6. Stone, K. J., and Strominger, J. L. (1971) *Proc. Natl. Acad. Sci. U.S.A. 68*, 3223−3227.
7. Drechsel, H., Stephan, H., Lotz, R., Haag, H., Zähner, H., Hantke, K., and Jung, G. (1995) *Liebigs Ann. Chem.* 1727−1733.
8. Gobin, J., Moore, C. H., Reeve, J. R., Jr., Wong, D. K., Gibson, B. W., and Horwitz, M. A. (1995) *Proc. Natl. Acad. Sci. U.S.A. 92*, 5189−5193.
9. Kunze, B., Jansen, R., Pridzun, L., Jurkiewicz, E., Hunsmann, G., Hofle, G., and Reichenbach, H. (1993) *J. Antibiot. 46*, 1752−1755.
10. Jansen, R., Kunze, B., Reichenbach, H., Jurkiewicz, E., Hunsmann, G., and Hofle, G. (1992) *Liebigs Ann. Chem. 4*, 357−359.
11. Anderson, B., Hodgkin, D. C., and Viswamitra, M. A. (1970) *Nature 225*, 233−235.
12. Selva, E., Montanini, N., Stella, S., Soffientini, A., Gastaldo, L., and Denaro, M. (1997) *J. Antibiot. 50*, 22−26.

13. Asencio, C., Pérez-Díaz, J. C., Martínez, M. C., and Baquero, F. (1976) *Biochem. Biophys. Res. Commun. 69*, 7−14.
14. Yorgey, P., Lee, J., Kordel, J., Vivas, E., Warner, P., Jebaratnam, D., and Kolter, R. (1994) *Proc. Natl. Acad. Sci. U.S.A. 91*, 4519−4523.
15. Bayer, A., Freund, S., and Jung, G. (1995) *Eur. J. Biochem. 234*, 414−426.
16. Vizán, J. L., Hernández-Chico, C., del Castillo, I., and Moreno, F. (1991) *EMBO J. 10*, 467−476.
17. San Millán, J. L., Kolter, R., and Moreno, F. (1985) *J. Bacteriol. 163*, 275−281.
18. Davagnino, J., Herrero, M., Furlong, D., Moreno, F., and Kolter, R. (1986) *Proteins: Struct., Funct., Genet. 1*, 230−238.
19. Yorgey, P., Davagnino, J., and Kolter, R. (1993) *Mol. Microbiol. 9*, 897−905.
20. Garrido, M. C., Herrero, M., Kolter, R., and Moreno, F. (1988) *EMBO J. 7*, 1853−1862.
21. Genilloud, O., Moreno, F., and Kolter, R. (1989) *J. Bacteriol. 171*, 1126−1135.
22. San Millán, J. L., Kolter, R., and Moreno, F. (1985) *J. Bacteriol. 163*, 1016−1020.
23. Li, Y.-M., Milne, J. C., Madison, L. L., Kolter, R., and Walsh, C. T. (1996) *Science 274*, 1188−1193.
24. Madison, L. L., Vivas, I. E., Li, Y.-M., Walsh, C. T., and Kolter, R. (1997) *Mol. Microbiol. 23*, 161−168.
25. Sinha Roy, R., Belshaw, P. J., and Walsh, C. T. (1998) *Biochemistry 37*, 4125−4136.
26. Belshaw, P. J., Sinha Roy, R., Kelleher, N. L., and Walsh, C. T. (1998) *Chem. Biol. 5*, 373−384.
27. Kelleher, N. L., Belshaw, P. J., and Walsh, C. T. (1998) *J. Am. Chem. Soc. 120*, 9716−9717.
28. Milne, J. C., Eliot, A. C., Kelleher, N. L., and Walsh, C. T. (1998) *Biochemistry 37*, 13250−13261.
29. Sinha Roy, R., Kim, S., Baleja, J. D., and Walsh, C. T. (1998) *Chem. Biol. 5*, 217−228.
30. Sambrook, J., Fritsch, E. F., and Maniatis, T. (1989) *Molecular Cloning: A Laboratory Manual*, 2nd ed., Cold Spring Harbor Laboratory, Cold Spring Harbor, NY.
31. McCafferty, D. G., Lessard, I. A. D., and Walsh, C. T. (1997) *Biochemistry 36*, 10498−10505.
32. Edelhoch, H. (1967) *Biochemistry 6*, 1948−1954.
33. Pace, C. N., Vajdos, F., Fee, L., Grimsley, G., and Gray, T. (1995) *Protein Sci. 4*, 2411−2423.
34. Senko, M. W., Hendrickson, C. L., Pasa-Tolic, L., Marto, J. A., White, F. M., Guan, S., and Marshall, A. G. (1996) *Rapid Commun. Mass Spectrom. 10*, 1824−1828.
35. Pohlner, J., Kramer, J., and Meyer, T. F. (1993) *Gene 130*, 121−126.
36. Guan, C., Li, P., Riggs, P. D., and Inouye, H. (1988) *Gene 67*, 21−30.
37. Betts, L., Xiang, S., Short, S. A., Wolfenden, R., and Carter, C. W., Jr. (1994) *J. Mol. Biol. 235*, 635−656.
38. Spence, J., and Georgopoulos, C. (1989) *J. Biol. Chem. 264*, 4398−4403.
39. Panaretou, B., Prodromou, C., Roe, S. M., O'Brien, R., Ladbury, J. E., Piper, P. W., and Pearl, L. H. (1998) *EMBO J. 17*, 4829−4836.
40. Kumar, S., Bathini, Y., Joseph, T., Pon, R. T., and Lown, J. W. (1991) *J. Biomol. Struct. Dyn. 9*, 1−21.
41. Plouvier, B., Bailly, C., Houssin, R., Rao, K. E., Lown, W. J., Henichart, J. P., and Waring, M. J. (1991) *Nucleic Acids Res. 19*, 5821−5829.
42. Perler, F. B. (1998) *Nat. Struct. Biol. 5*, 249−252.
43. Porter, J. A., Young, K. E., and Beachy, P. A. (1996) *Science 274*, 255−259.
44. Lowe, J., Stock, D., Jap, B., Zwickl, P., Baumeister, W., and Huber, R. (1995) *Science 268*, 533−539.
45. Lipscomb, W. N., and Strater, N. (1996) *Chem. Rev. 96*, 2375−2433.
46. Xiang, S., Short, S. A., Wolfenden, R., and Carter, C. W., Jr. (1997) *Biochemistry 36*, 4768−4774.
47. Sander, E. G., and Heeb, M. J. (1971) *Biochim. Biophys. Acta 227*, 442−452.
48. Pascal, R. A., Jr., Trang, N. L., Cerami, A., and Walsh, C. (1983) *Biochemistry 22*, 171−178.
49. Kjeldgaard, M., Nyborg, J., and Clark, B. F. (1996) *FASEB J. 10*, 1347−1368.

BI982975Q